UPPSALA UNIVERSITET

Independent Project at the Department of Earth Sciences
Självständigt arbete vid Institutionen för geovetenskaper
2021: 15

Turbulence Intensity During Low-Level Jets in the Baltic Sea

Turbulensintensitet i samband med Low-Level Jets över Östersjön

August Thomasson

DEPARTMENT OF EARTH SCIENCES
INSTITUTIONEN FÖR GEOVETENSKAPER

Independent Project at the Department of Earth Sciences
Självständigt arbete vid Institutionen för geovetenskaper
2021: 15

Turbulence Intensity During Low-Level Jets in the Baltic Sea

Turbulensintensitet i samband med Low-Level Jets över Östersjön

August Thomasson

Published at Department of Earth Sciences, Uppsala University (www.geo.uu.se), Uppsala, 2021

Abstract

Turbulence intensity during Low-Level Jets in the Baltic Sea
August Thomasson

Low-level jets (LLJs) are local wind speed maximums in the atmospheric boundary layer. In the Baltic Sea, LLJs are frequently occurring in spring and summer. It is an important phenomena to consider for wind energy parks, and changes in turbulence during the jets can effect the efficiency of said parks. In this study, the effect that offshore LLJs have on turbulence intensity (TI) is analysed and the goal is to understand if TI significantly changes as the jets form, and if the changes are different above and below the core. The theory of shear sheltering predicts that turbulence decreases below the core of a LLJ, and it has been experimentally tested previously with various results. However, turbulence characteristics above the core of a LLJ has not been studied before. LiDAR measurements of wind speed and TI profiles, up to 300 m, from the island of Östergarnsholm in the Baltic Sea are used. The measurements are from the period 2016-2020 and are limited to a sector with unobstructed line-of-sight to the ocean. Complete LLJ-events, which includes non-LLJ profiles before and after the actual jets, are analysed. The LLJs are found to appear in low TI conditions related to stable stratification. Mean TI increases with $38 - 47\%$ above the core as the jets appear, and then returns to approximately the initial values after the jets disappear. Below the core, mean TI instead decreases with $14 - 19\%$ during the jets, which is compatible with the theory of shear sheltering. For future studies it is recommend to choose a location with larger unobstructed line-of-sight to the ocean, further optimise the LLJ-finding algorithm and also analyse other turbulent quantities.

Keywords: Low-Level Jet, Turbulence intensity, Shear sheltering, LiDAR, Baltic Sea

Degree Project C in Meteorology, 1ME420, 15 credits, 2021
Supervisor: Christoffer Hallgren
Subject reader: Erik Sahlée
Department of Earth Sciences, Uppsala University, Villavägen 16, SE-752 36 Uppsala (www.geo.uu.se)

Sammanfattning

Turbulensintensitet i samband med Low-Level Jets över Östersjön
August Thomasson

Vindmaxima på låg höj (LLJ, för *eng. Low-level jets*) är lokala vindhastighetsmaximum i det atmosfäriska gränsskiktet. I Östersjön är LLJs vanliga, framförallt på våren och sommaren. Det är ett viktigt fenomen att beakta för vindkraftsparker, och turbulensförändringar i samband med LLJs kan påverka effektiviteten av vindkraftverk. I denna studie analyseras effekten som LLJs över havet har på turbulensintensiteten (TI) och målet är att förstå om TI förändras när strömmarna bildas, och om förändringarna är olika ovan och under kärnan. En teori förutspår att turbulens minskar under kärnan i en LLJ, s.k. skjuvningsblockering (*eng. Shear sheltering*), och den har testats tidigare med varierande resultat. Turbulens ovanför kärnan i en LLJ har dock inte studerats tidigare. LiDAR-mätningar av vindhastighets och TI-profiler, upp till 300 m, vid ön Östergarnsholm i Östersjön används. Mätningarna är från perioden 2016-2020 och är begränsade till en sektor med fri siktlinje mot havet. Kompletta LLJ-event, vilket inkluderar icke-LLJ-profiler före och efter själva strömmen, analyseras. Resultatet visar att LLJs förekommer vid låga TI-förhållanden relaterade till stabil skiktning. Medel TI ökar med $38 - 47\%$ över kärnan när strömmarna dyker upp och återgår sedan till ungefär de ursprungliga värdena efter att strömmarna försvunnit. Under kärnan minskar medel TI istället med $14 - 19\%$ i samband med strömmarna, vilket är förenligt med skjuvningsblockerings-teorin. För framtida studier är det rekommenderat att välja en plats med större fri siktlinje till havet, ytterligare optimera identifikationen av kompletta LLJ-event och även analysera andra variabler för att karakterisera turbulensen.

Nyckelord: Low-Level Jet, Turbulensintesitet, Shear sheltering, LiDAR, Östersjön

Examensarbete C i meteorologi, 1ME420, 15 hp, 2021
Handledare: Christoffer Hallgren
Ämnegranskare: Erik Sahlée
Institutionen för geovetenskaper, Uppsala universitet, Villavägen 16, 752 36 Uppsala (www.geo.uu.se)

Hela publikationen finns tillgänglig på www.diva-portal.org

Contents

1. Introduction

During the current global climate state, demand for renewable energy is growing. For many countries this means a rapid increase in wind power production. A large part of this development will be in offshore wind energy, which generally have higher wind speeds, thus more electricity generated, than onshore wind energy (Bilgili et al. 2011). In the Baltic Sea, offshore wind energy is mainly used by Germany and Denmark, and too a lesser extent Sweden and Finland (Ramírez et al. 2020). In Sweden, wind energy is planed too make up 43% of the country's total electricity generation in 2040, compared to 11% in 2018 (Swedish wind energy association 2019). Being a large semi-enclosed basin, different weather conditions connected to the proximity to the shore creates deviations from the normal wind profile in the Baltic Sea. For example, sea breeze and low-level jets (Hallgren et al. 2020, Svensson et al. 2019).

Low-level jets (LLJs) are local wind speed maximums in the atmospheric boundary layer (see example in figure 1). The phenomena's occurence and large scale characteristics (such as strength, direction and variability) have been extensively studied before and is well understood, both onshore (Blackadar 1957, Bonner 1968, Holt 1996, Parish 2000, Banta et al. 2002, Baas et al. 2009) and offshore (Andreas et al. 2000, Tuononen et al. 2017, Svensson et al. 2019, Hallgren et al. 2020). In the Baltic Sea, LLJs are a common phenomena with a peak frequency of around 20% in the spring (Tuononen et al. 2017, Svensson et al. 2019) or even as much as 60% in spring depending on yearly variability and exact definition of the jets (Hallgren et al. 2020). It is important to consider the jets when analysing wind power potential in the basin (Hallgren et al. 2020).

Small scale characteristics of LLJs (i.e. turbulence), on the other hand, is much less understood. Hunt & Durbin (1999) describes different flows with different velocity fields. These fields are separated by layers with significant variations in vorticity. According to Hunt & Durbin (1999), depending on the flow situation, the velocity fields can "mutually exclude each other across the interface" thus reducing turbulence at the interface, a situation the authors call *shear sheltering*. Hunt & Durbin (1999) calculated that detached large eddies moving towards a shear zone can be suppressed if they move with a horizontal velocity close to the mean velocity of the flow and have appropriate size.

The application of shear sheltering on LLJs, which by definition has large shear around its core, as been studied before with inconclusive results (Smedman et al. 2004, Prabha et al. 2008, Duarte et al. 2012). Smedman et al. (2004) analyses offshore LLJs during stable conditions and found that low frequency turbulence is suppressed, in accordance to the theory. Prabha et al. (2008) analyses onshore nocturnal LLJs, the former above forest canopy and the latter above a wetland, and they found similar results: turbulence decreases below the LLJ-core. On the other hand, Duarte et al. (2012) analyses nocturnal onshore LLJs above plains and found no evidence of decreased turbulence during the jets.

Turbulence is also an important factor to consider while analysing wind power potential. Increased turbulence can be problematic for turbines, potentially lowering their lifetime and decreasing efficiency (Tuononen et al. 2017). On the other hand, increased turbulence can also lead to less wakes behind the turbines, thus increasing efficiency of large wind energy parks (Dörenkämper et al. 2015, Nagarada Gadde & Stevens 2020). Large eddy simulations show that LLJs can increase efficiency of wind parks, due too faster wake recovery and larger kinetic energy flux, depending on the height of the LLJ (Nagarada Gadde & Stevens 2020).

This means that changes in turbulence during LLJs can both be negative and positive for offshore wind energy parks. Therefore, a more fundamental understanding of turbulence characteristics during LLJs is valuable (Tuononen et al. 2017). One way to achieve that is to answer the question of how the vertical turbulence intensity profile behaves during LLJs. Do the existence of the jets lead to a change in the turbulence intensity or not. And if they do so, is it due to shear sheltering.

The main goal of this study is therefore to analyse the vertical profile of turbulence intensity during offshore LLJ-events in the Baltic Sea, and to find out whether or not the results are compatible with the shear sheltering theory. Previous studies on turbulence during LLJs (Smedman et al. 2004, Prabha et al. 2008, Duarte et al. 2012) focused on the zone below the core of the jet and, to our knowledge, no studies have analysed turbulence above the core of a LLJ. That is why this study also aims to answer if the effects of LLJs on turbulence intensity is uniform within the vertical profile or if the changes are different above and below the core of the jet.

This report is structured into five sections. First, the theory of low-level jets, the instrument used (LiDAR) and shear sheltering is presented. Then a description of the method follows, which includes identifying complete LLJ-events and analyses of turbulence intensity. The next two sections presents and discusses the results, future recommendations and errors. Concluding remarks are presented in the final section.

2. Theory

2.1 Low-Level Jets

A wind field with a local wind speed maximum in the lower kilometer of the atmosphere is called a low-level jet (LLJ), see example profile in figure 1. There are no generally accepted criteria for a LLJ, but often a threshold for how much the maximum exceeds wind speeds both above and below it is used. Usually this threshold is set to $1-2$ m/s. The criteria can also be related to the persistence of the LLJ in time, in combination with a wind speed criteria.

For example, Svensson et al. (2019) uses a 1 m/s (as well as 2 m/s, to compare results) for how much the maximum has to exceed the wind speed at any point above it, as well as a persistence of at least 3 hours. Relative limits can also be used; Baas et al. (2009) uses 2 m/s falloff (if the wind speed of core is less than 10 m/s) and 20% falloff (if the wind speed of core is more or equal to 10 m/s) as a criteria. While a height limit is necessary to define, since the LLJs are local maximums, there are no consensus on any specific limit. The vertical extent of any study is often confined to the reach of the instrument or model used. Of course, radiosonde-measurement or numerical simulation have very high vertical reach but a limit is often defined to approx. $300-1000$ m.

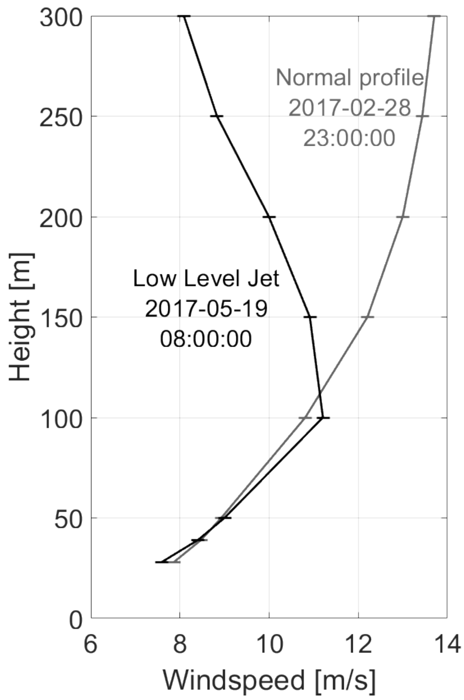

Figure 1. Example of a low-level jet and a normal wind profile above Östergarnsholm at two different occasions. The markers indicate the different measurement heights

The formation of LLJs can be contributed to several different events. Over land LLJs often form due to frictional decoupling at night, as a stable lapse rate leads to less vertical mixing. This decreases turbulence, allowing the wind speed to increase. These jets are often called nocturnal jets (Blackadar 1957). Over oceans a similar frictional decoupling can occur when air warmed over land moves over cooler water, thus leading to similar stable conditions (Kaellstrand 1998). LLJs can also be induced by thermal winds caused by temperature gradients (Holt 1996) or synoptic weather events (Parish 2000).

In the Baltic Sea, LLJs have been extensively studied before. It is clear that LLJs are a common occurrence in the basin. Svensson et al. (2019) found a peak occurrence at Östergarnsholm, Sweden in May with $18-27\%$. Similar numbers were found by Tuononen et al. (2017) with occurrence of around 20% in spring and summer at Utö, Finland, with a maximum occurrence of around 60% in May found by Hallgren et al. (2020) at the same location. The large variation in occurrence between studies is both due to different criterias used to define the jets and yearly variability, where the yearly variability is contributed to large scale synoptic weather patterns influencing the formation of LLJs (Hallgren et al. 2020).

2.2 ZephIR 300 LiDAR

By focusing a laser beam at a specific height and measuring the backscatter, a LiDAR (Light Detection And Ranging) uses Doppler-shift analysis to calculate characteristics of the airflow. A ZephIR 300 LiDAR (ZX Lidars, UK) is a 30° conically scanning, continuous-wave LiDAR; it scans a horizontal cross-section of a cone at each specific height. The raw data is measured at 50 Hz, but is presented in 10-minute averages; which includes wind speed, u, wind direction, wd and turbulence intensity TI (defined as the ratio of standard deviation of wind speed to the wind speed, σ_u/u). Measurements can be done at up to 10 user chosen heights, between 10 and 300 meters.

Being a continuous-wave type, the LiDAR has better focus at shorter distances, which leads to a larger measurement volume at higher heights. The effect is noticeable; 50% of the measurement volume lies within ± 80 m at 300 m but only within ± 0.7 m at 28 m (Svensson et al. 2019). Also the radius of the scan circle increases considerably with height. This leads to uncertainty in the measurements (Svensson et al. 2019).

Both Sathe et al. (2011) and Svensson et al. (2019) compare the LiDAR's measurements to a nearby weather tower and found that the LiDAR in general has good correlation with the tower. For wind speed and direction, Svensson et al. (2019) found a very good agreement and a correlation of $r^2 = 0.99$. For momentum flux, the correlation was not as good, with $r^2 = 0.68$, probably due to uncertainty in magnitude. Looking at time series, however, the authors found a clear relationship. The ZephIR LiDAR also underestimates the wind speed standard deviation, and therefore TI, due to the larger measurement volumes at higher heights mentioned previously when comparing to measurements of a nearby weather tower (Sathe et al. 2011). Svensson et al. (2019) concludes that the LiDAR can be used to analyse turbulent quantities up to at least 100 m reliably, and that methods for analysis at higher heights has to take this into account.

2.3 Shear sheltering

Shear sheltering is a term coined by Hunt & Durbin (1999). According to the theory, large detached eddies traveling towards a zone of high shear can be fully blocked from passing through the zone, if certain conditions of eddy size and velocity is met. Thus suppressing, or sheltering, turbulence in the shear zone. The phenomena is well documented within fluid-engineering, with several direct numerical simulations (e.g. Jacobs & Durbin (2001), Brandt et al. (2004)) and experimental (e.g. Hernon et al. (2007)) studies using shear sheltering.

Applying shear sheltering theory to atmospheric physics, and low-level jets specifically, was first done by Smedman et al. (2004). Using wind and turbulence profile data, by means of radio soundings and tower measurements from two marine sites in the Baltic Sea they found that low frequency turbulent energy in the surface layer is suppressed in the presence of LLJs. A previous study, Smedman et al. (1997) found similar results, though no connection to shear sheltering was done.

By definition LLJs have large wind shear around its core, which presents an apparent paradox; since turbulence often is proportional to shear, how can LLJs suppress turbulence (Smedman et al. 2004)? Smedman et al. (2004) argue that this result is due to the shear sheltering phenomena, using the same theory outlined by Hunt & Durbin (1999). Eddies of appropriate size and horizontal velocity close to the mean wind speed above the shear zone is prevented from passing through the LLJ.

Prabha et al. (2008) applied the same theory to nocturnal LLJs above a forest canopy in Maine, USA using a sodar. Analysing wind profile and eddy covariance data they found that events with strong LLJs and wind shear were associated with strong shear sheltering. On the other hand, during cases with low wind shear and weak to no LLJs no shear sheltering was observed. Prabha et al. (2008) found that cases with low shear sheltering is characterized by high turbulence intensity (σ_u/u in range $0.4 - 1.0$). On the other hand, cases with high shear sheltering is characterized by low turbulence intensity ($\sigma_u/u \approx 0.3$), suggesting that high shear sheltering suppresses *TI* (see Smedman et al. (2004) and Prabha et al. (2008) for definition of high and low shear sheltering).

Duarte et al. (2012) revisits shear sheltering theory by analysing wind profile and turbulence data of nocturnal LLJs above plains in Oklahoma, USA, using sodar and sonic anemometer measurements. Contrary to previous studies they show that strong jet shear conditions leads to increased turbulence and surface fluxes, suggesting that shear sheltering is not present during LLJs. Therefore, the authors speculate that shear sheltering is not normally applicable to fluid mechanics in the boundary layer over land. However, they do point out that the absence of shear sheltering in their study could be contributed to the eddies not meeting the proposed criteria of scale and speed by Hunt & Durbin (1999).

Though low-level jets have strong shear both above and below the core, shear sheltering theory is only applied to the bottom shear layer (Smedman et al. 2004, Prabha et al. 2008, Duarte et al. 2012). Knowledge about how turbulent quantities are effected by the shear zone above the LLJ-core is lacking and, to our knowledge, this study is the first to analyse turbulence above the jets.

3. Method

3.1 Data

The data used in this study comes from a ZephIR 300 LiDAR (ZX Lidars, UK) placed on Östergarnsholm's field station which has been used in previous studies (Rutgersson et al. 2020, Svensson et al. 2019, Hallgren et al. 2020). Östergarnsholm is a small island approximately 4 km east of Gotland in the Baltic Sea. At its location on the southern most tip of a small land tongue, the LiDAR has an unobstructed line of sight to the open ocean in approximately $45-220°$, except for a small hut in $110-150°$. In the direction of $220-295°$ Gotland lies, and from $295-45°$ the island it self lies. These sectors are illustrated in figure 2.

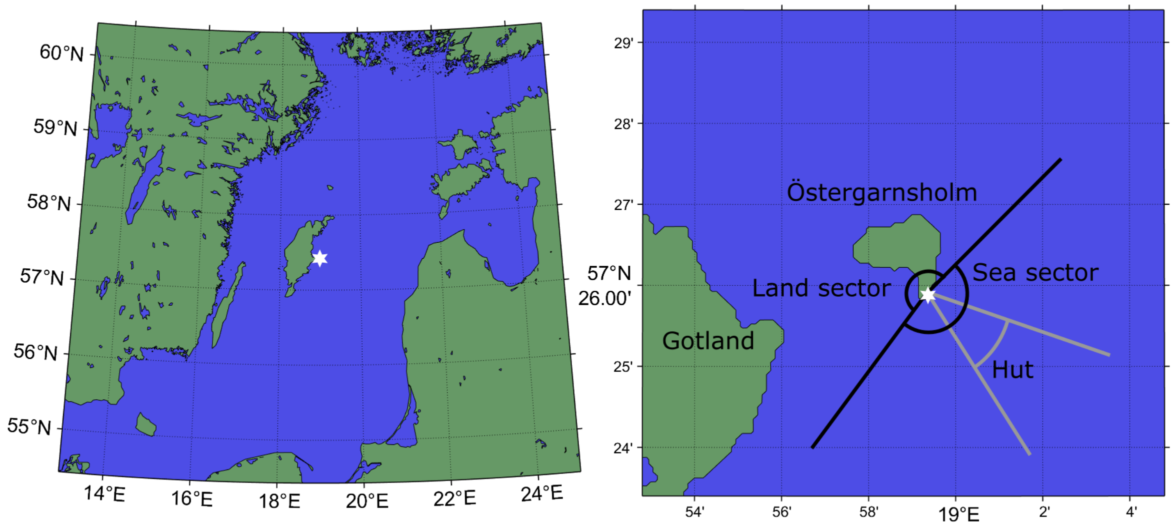

Figure 2. Left: Östergarnsholm's location in the Baltic Sea marked with a white star. **Right**: Östergarnsholm with the LiDAR location marked with a white star as well as the different sectors

The goal is to analyse offshore LLJs, why the direction is limited to the open sea, i.e. $45-220°$. Air flowing over land has other turbulence characteristics compared to airflow over the ocean. The small hut in the direction of $110-150°$ constitutes an obvious source of error. The effect of the hut on turbulence intensity profiles is unknown. Therefore, profiles with any measurement with wind direction outside the accepted direction of $45-110°$ and $150-220°$ are not considered for this study.

The data includes wind speed, wind direction and turbulence intensity. The instrument was deployed from the 8th of December 2016 to the 24th of June 2020. During that time-period the instrument measured almost continuously with only minor breaks for maintenance and calibration; exceptions being during 2019 from February through April, as well as August through November in which the LiDAR was inactive. During 2016 and 2017 the data was presented in 30 minute means. This was later changed to 10 minute means from 2018 and onwards.

The LiDAR measured at heights of 28, 39, 50, 100, 150, 200, 250 and 300 m above sea level, though some small change occurred throughout the years. See markings in figure 1. One period during 2019 the 250 m level was skipped and the 28 m level measured at 29 m instead. Another short period, an additional measurement at 40 m was used.

In some instances the LiDAR measures wind direction shifted by $\pm 180^\circ$, since the sign of the backscatter signal cannot be distinguished, i.e. it is homodyne. To correct for this error, the LiDAR chooses the direction which is closest to the direction measured by an independent anemometer attached to the LiDAR. By comparison to a nearby weather station, Svensson et al. (2019) found that approximately 1.7% of the total data still is shifted by $\pm 180^\circ$ after the LiDAR's internal correction.

3.2 Quality control

The data includes several data points which are missing or are incorrect. To check for erroneous wind speed data points, the difference between consecutive height measurements for each profile is analysed. If there exists a vertical change, both decrease or increase, of approximately 4 m/s or more, the profile is manually checked. If obviously erroneous the entire profile is removed.

The same height-difference analysis is done for *TI* profiles. Profiles with a vertical change of approximately 0.7 or more is manually checked. *TI* profiles are more variable than wind speed profiles and erroneous profiles are therefore not as easy to manually remove. Still, some profiles are possible to remove manually. For example, if a single point is much higher or lower than the others or if the values are oscillating back and forth.

As mentioned in section 3.1, the LiDAR is homodyne. Therfore, the wind direction profiles has to be checked for a shift of $\pm 180^\circ$. Profiles with a vertical wind veer of $170 - 190^\circ$ between two consecutive heights are check manually. If obviously affected by the homodyne problem they are removed. However, this method only finds profiles for which at least one point is correctly measured by the LiDAR. If the entire profile is shifted by $\pm 180^\circ$, comparison to external measurements has to be done, which is not possible in this study. But since only approximately 1.7% of profiles are affected by this (Svensson et al. 2019), and some of them can be removed, this should not affect the results.

The last quality control is done by removing profiles with three or more missing measurements, since they are deemed unreliable to use in the analysis. The quality control leads to removal of 11.96% of the profiles within the selected wind direction, a large majority (11.93%) being removed when checking for profiles with three or more missing values.

Finally, data from 2018 and onwards is converted from 10-minute means to 30-minute means in order to get comparable data. LLJs are events with a persistence of several hours Hallgren et al. (2020), why 30-minute means of wind speed and turbulence intensity is sufficient for this study.

3.3 Identifying low-level jet events

The algorithm used to find LLJ-events is described in this section. It is partly based on the algorithm used by Tuononen et al. (2017), consisting of two parts: a main criteria and a threshold criteria. The main criteria identifies LLJ-profiles and the threshold criteria ensures coherent LLJ-events.

The main criteria for this study is applied as follows: first, all profiles with a local wind speed maximum at either 100 or 150 m are identified. They are then checked according to the LLJ-criteria. If the core wind speed, u_{core}, is less than 10 m/s, then at least one measurement above and below the core has to have a wind speed an absolute value less than u_{core}. If instead u_{core} is equal or more than 10 m/s, a relative threshold is used. A profile that meets these criteria is labeled a LLJ-profile.

Then a threshold criteria is applied to find consecutive LLJ-profiles. In Tuononen et al. (2017), this includes four thresholds that checks for consistent height, wind speed, wind direction and time difference between any consecutive LLJ-profiles. As mentioned previously, this study is already limited in height and wind velocity. Therefore, only a temporal threshold is used to define LLJ-events. The time difference between two consecutive LLJ-profiles can be a maximum of 1.5 hours, i.e. allowing for two missing profiles. The minimum total length of any LLJ-event is also defined. Profiles that fits this threshold criteria are labeled a LLJ-event.

In order to find non-LLJ profiles before and after a LLJ-event, a simple falloff criteria is applied. First the same number of profiles before and after the event, as the number of profiles of that event, are identified. These profiles are then tested so that they do not have any vertical change in wind speed less than -0.5 m/s (i.e. allowing for any positive shear but only slight negative shear). This criteria excludes all but the weakest LLJs, and allows for flexibility in the profiles appearance. Then a similar temporal threshold criteria is applied to the non-LLJ profiles. The largest gap between the non-LLJ and LLJ-event is 3 hours, which allows for six transition profiles. The time difference between two consecutive non-LLJ-profiles can be a maximum of 1.5 hours. Any event that has at least one non-LLJ profile both before and after according to these criteria is labeled a complete LLJ-event.

The choice of values in the main and threshold criteria for a LLJ-profile is rather arbitrary. Too evaluate how reliable the algorithm is at finding complete LLJ-events, it is run with several different criterias. This evaluation covers most criteria used in previous studies (Blackadar 1957, Bonner 1968, Andreas et al. 2000, Smedman et al. 2004, Prabha et al. 2008, Baas et al. 2009, Tuononen et al. 2017, Svensson et al. 2019, Hallgren et al. 2020) and are as follows; 1 m/s & 10%, 1.5 m/s & 15% and 2 m/s & 20% as well as a minimum LLJ-event length of 2, 2.5 and 3 hours. The results are presented in the Table 1.

Table 1. The number of LLJ-events, complete LLJ-events, profiles before LLJ, LLJ-profiles and profiles after LLJ depening on the criteria used in the identifying-algorithm. The criteria are presented in the format; Abs (if $u_{core} < 10$ m/s), rel (if $u_{core} \geq 10$ m/s), minimum length of LLJ-event

Criteria	LLJ-events	Complete LLJ-events	Profiles before LLJ	LLJ-profiles	Profiles after LLJ
1m/s, 10%, 2h	72	21	106	205	97
1m/s, 10%, 2.5h	54	19	100	195	93
1m/s, 10%, 3h	43	16	90	178	82
1.5m/s, 15%, 2h	49	11	55	106	57
1.5m/s, 15%, 2.5h	38	10	52	101	55
1.5m/s, 15%, 3h	31	8	46	90	47
2m/s, 20%, 2h	24	9	45	87	49
2m/s, 20%, 2.5h	19	7	39	77	44
2m/s, 20%, 3h	17	7	39	77	44

From Table 1 it is clear that, rather expected, stricter main criteria leads to less LLJs found. A longer minimum length also leads to less LLJs found, but the effect is not as large. In this study, it is important to use a data-set as large as possible to minimize errors when analysing means. On the other hand, a minimum length of only two hours would lead to the possibility of a LLJ-event consisting of only two profiles (since a gap of 1.5 hours is allowed). The criteria of 1 m/s, 10%, 2.5 h is therefore a good compromise, leading to a large number of complete events. It also ensures that each LLJ-event consists of at least three profiles.The complete events are controlled manually to ensure that incorrect profiles are found by the algorithm. In summary, the criteria for a complete LLJ-event used in this study are:

- Local wind speed maximum, u_{core}, at 100 or 150 m
- If $u_{core} < 10$ m/s, at least one point above and below the core has to be at least 1 m/s less than u_{core}
- If $u_{core} \geq 10$ m/s, at least one point above and below the core has to be at least 10 % less than u_{core}
- Non-LLJ profile if $\Delta u > -0.5$ m/s between consecutive heights
- Time difference between consecutive profiles ≤ 1.5 hours
- The total length of a LLJ-event ≥ 2.5 hours
- Time difference between non-LLJ and LLJ < 3 hours
- At least one non-LLJ profile before & after a LLJ-event

3.4 Normalization & uncertainty

As Hallgren et al. (2020) notes, LLJs at Östergarnsholm can occur during many different weather conditions, from calm to stormy. This leads to different events having different initial turbulence intensity and initial wind speeds. Analysis with different events, for example by computing means, may have uncertainty due to different initial conditions. In an attempt to eliminate this bias all event's *TI* measurements are normalized based on the turbulence intensity as follows:

For each height, the mean *TI* during a LLJ-event is used as the normalization factor. Each individual measurement for that complete LLJ-event (including the profiles before and after) and at that specific height is then divided by the normalization factor. The result is that each measurement effectively represents the relative deviation from mean *TI* during the LLJ-event. The method is repeated for each complete event. The wind speed measurements are normalized the same way, but with the mean wind speed of each event. The ZephIR LiDAR does not provide any uncertainty in the measurements. Instead the measurements are assumed to be Gaussian distributed with the arithmetic mean, $\bar{x}$, assumed to be the expected value with the standard deviation σ_x. For calculations of the mean in any variable a 95% confidence interval is assumed to be $\bar{x} \pm 1.96\sigma_{\bar{x}}$ where $\sigma_{\bar{x}} = \sigma_x/\sqrt{n}$ and n is the number of measurements.

The normalized data is presented on logarithmic scale, in order to easier visualize the data. If the normalized data is $\bar{x}$ with 95% confidence interval error of $\delta\bar{x}$, the logarithmic normalized data is $\log_2 \bar{x}$ and standard error propagation leads to the error seen in equation 1.

$$\delta \log_2 \bar{x} \approx \left| \frac{1}{\ln 2} \frac{\delta \bar{x}}{\bar{x}} \right| \tag{1}$$

3.5 Analysis of turbulence intensity

The analysis of *TI* characteristics during complete LLJ-events is split into three parts. Firstly, the *TI* data during LLJs is compared to the entire data set (but with the same restrictions on wind direction, see section 3.1) in order to identify any patterns or general characteristics. In practice, scatter plots of *TI* versus wind speed and *TI* versus shear (where shear is defined as the change in wind speed divided by the change in height, $S = \Delta u/\Delta h$, for two adjacent heights) suits this analysis well. These scatter plots are devided into the two height ranges of interest, i.e. below (< 100 m) and above (> 150 m) the LLJ-core.

Secondly, the difference in *TI* between the LLJ-profiles and the before/after profiles is analysed by calculating the mean vertical profile with 95% confidence interval, both for the actual measurements and for the normalized measurements. The distribution of the normalized measurements is also analysed by means of histograms split into the same two height ranges of interest.

Lastly, the evolution of *TI* for the complete events is analysed by plotting continuous time series. This is done only for the normalized data, so that any general trend in changes of *TI* during the jets are easier visualized.

4. Results

4.1 Low-level jets in relation to the sea sector

In this section, *TI* during the jets is compared to *TI* of the entire data set. From the main criteria used (1 m/s, 10%) a total of 994 LLJ profiles are found, out of these 495 occurred during LLJ-events (with minimum length of 2.5 hours). 195 of these occurred during complete events, i.e LLJ-events with at least one non-LLJ profile before and after (see section 3.3). With 13906 total profiles in the given wind direction and time period, the frequency of LLJ-profiles within a LLJ-event is 3.3% and within a complete LLJ-event is 1.4%. For all analyses, only profiles within complete LLJ-events are used.

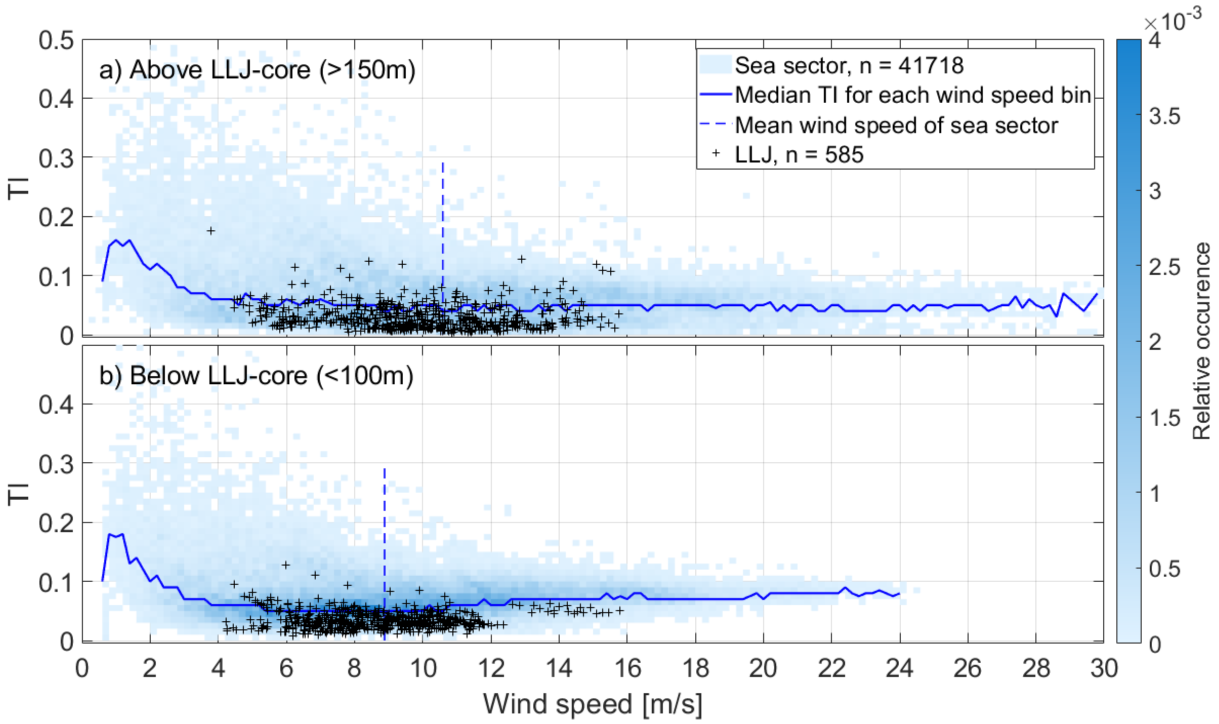

Figure 3. Scatter plot of *TI* as a function of windspeed. The background scatter distribution represents all quality controlled data within the used wind direction range for measurements at 200, 250 and 300 m (**a**) or 29, 38 and 50 m (**b**). Bin size is 0.02 m/s along the x-axis and 0.01 along y-axis. The continuous blue line represent median *TI* for each wind speed bin, while dashed blue line marks the mean wind speed at that height range. Note that 585 LLJ data points comes from 195 LLJ profiles at three different heights

Scatter plots of *TI* against both wind speed and shear, showing the location of *TI* during LLJs in relation to the entire sea sector is presented in figure 3 & 4. In both figures a majority of LLJ data points are below the median *TI*, suggesting in general low *TI* during the jets. There is also no clear correlation between either *TI* and wind speed or *TI* and shear within the LLJ measurements.

Figure 3 also shows that the LLJ data is evenly distributed around the mean wind speed, except for a small number of outliers in the 14 − 16 m/s range below the core. Figure 4a) show how shear above the jet core predominately is negative, while figure 4b) show how shear below the core is positive. This follows the definition of low-level jets (see figure 1). Above the jet core, LLJ-events coincides with the most extreme negative shear measurements, suggesting that the phenomena is the main contributor to extreme negative shear in the height range. The profiles with these extreme values have been manually checked and the conclusion is that they are correct.

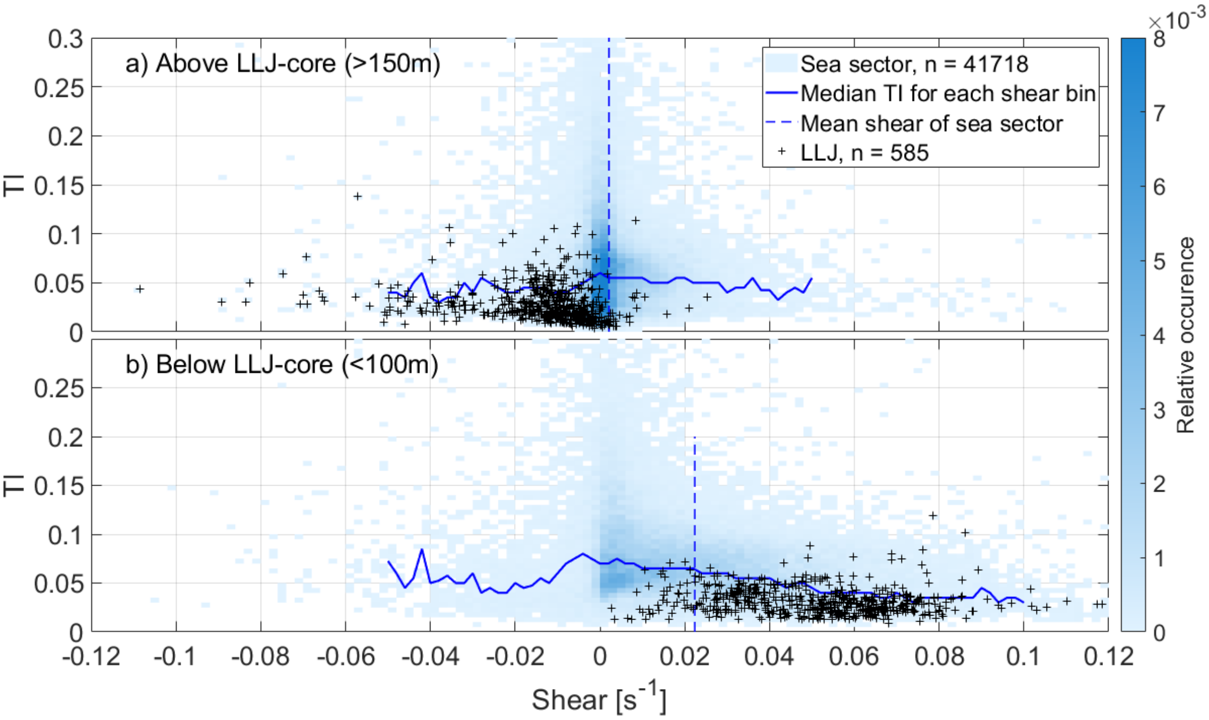

Figure 4. Scatter plot of *TI* as a function of shear. The background scatter distribution represents all quality controlled data within the used wind direction range for measurements at 200, 250 and 300 m (**a**) or 29, 38 and 50 m (**b**). Bin size is 0.002 s^{-1} along the x-axis and 0.005 along y-axis. The continuous blue line represent median *TI* for each shear bin, while dashed blue line marks the mean shear at that height range. Note that 585 LLJ data points comes from 195 LLJ profiles at three different heights

4.2 *TI* before, during and after LLJ

In figure 5a), the vertical profiles of mean wind speed before, during and after LLJs are presented. We see that LLJs have a higher mean wind speed below the core, though there is overlap in confidence interval. Comparing before and during the jets, the overlap of the confidence interval is large.

In figure 5b), on the other hand, vertical profiles of mean *TI* before, during and after LLJs are presented. Above the core, *TI* during the jets is significantly higher compared to before and after, except at 300 m where there is a slight overlap. At 200 & 250 m the differences are well outside the 95% confidence interval. For example, at 200 m the initial mean *TI* is 0.021 ± 0.003. As the LLJs forms mean *TI* increases to 0.030 ± 0.003, but ones the jets disappear mean *TI* returns to similar values; 0.019 ± 0.003.

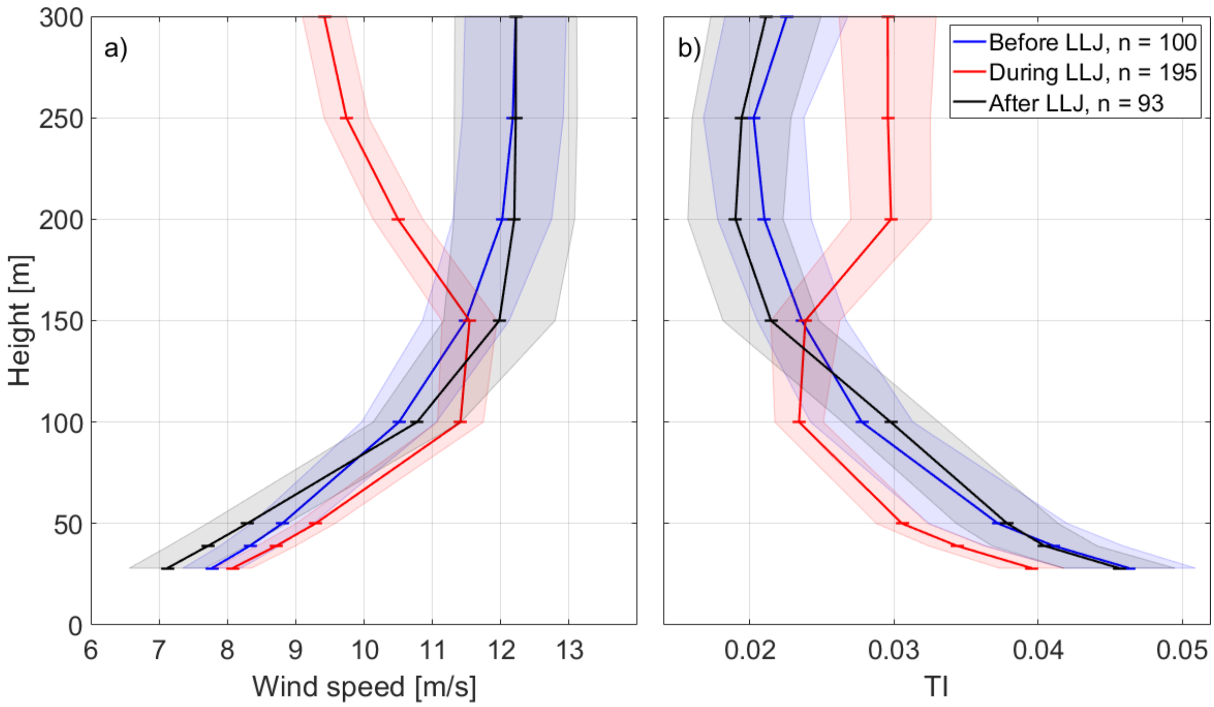

Figure 5. Vertical profile of the mean wind speed (**a**) and mean *TI* (**b**) for before, during and after the 19 low-level jets analysed. The shaded area represents a 95% confidence interval, based on assumed Gaussian distributed data. Please note that the x-axis are not starting at the origin

Below the core, the difference is not as large. Before LLJs, mean *TI* is consistently 0.06 above mean *TI* during the jets, though the difference is on the edge of the 95% confidence interval. Similarly, mean *TI* after the jets is between $0.06 - 0.07$ larger than mean *TI* during LLJs. For this case, the difference actually is outside the 95% confidence interval at 50 & 38 m, and just on the edge at 29 m. At 50 m, for example, initial mean *TI* is 0.037 ± 0.005, then 0.031 ± 0.002 during the jets and finally 0.038 ± 0.004 after the LLJs. This shows that mean *TI* below the core decreases in the presence of a LLJ.

4.2.1 Normalized data

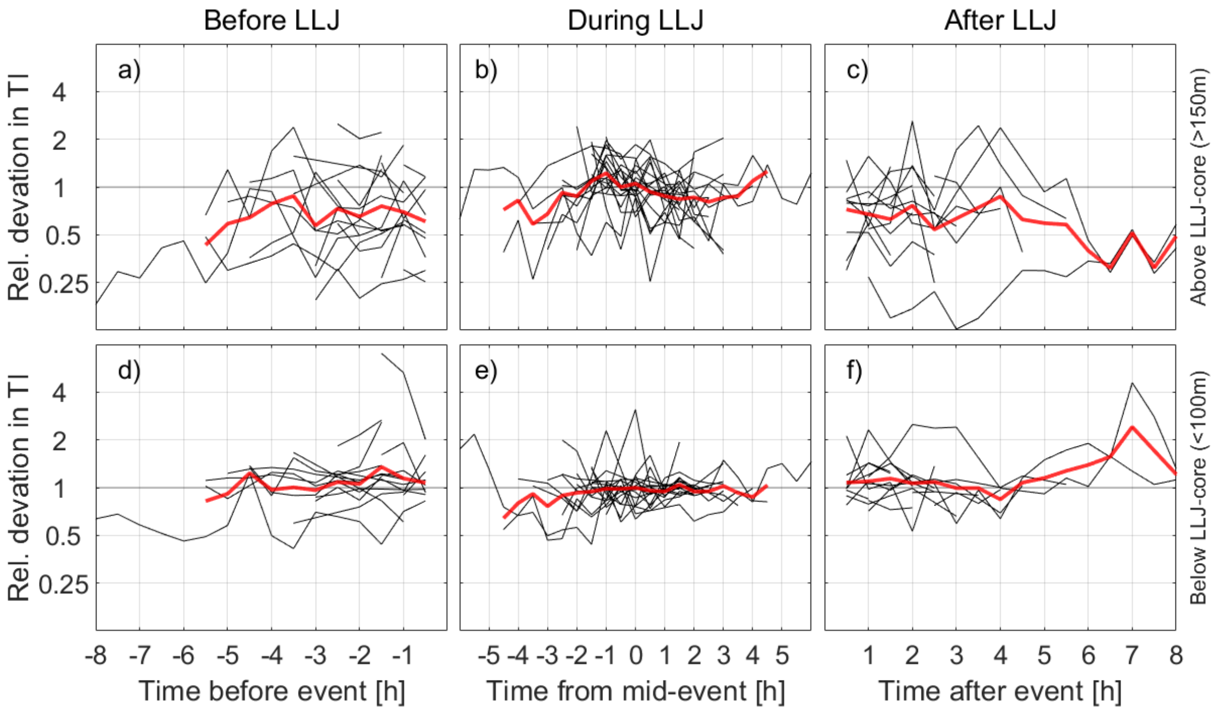

Figure 6. The evolution of normalized *TI* in time for each complete LLJ-event. Each black line represents the mean normalized *TI* for the two height-ranges of interest for one complete LLJ-event before (**a, d**), during (**b, e**) and after the LLJ (**c, f**). The top row (**a, b, c**) include the area above the core. The bottom row (**d, e, f**) include the area below the core. The red line represents the mean of all the black lines, but do note that this is not a representative mean since each complete LLJ-event have different length

In this section the results for the normalized data is presented. Figure 6 visualizes the evolution in time for each complete LLJ-case. In the figure each line represents one event and the red line is the mean of the events. Note that each event have different length, which means that the red line is the mean of different amount of events at each time step. Above the core, the variation is large, but the mean *TI* increases during LLJs. Below the core, on the other hand, *TI* is in general slightly large before and after the LLJ, though for some cases the opposite is true. The variation is smaller below the core. From figure 6, note that *TI* have larger variability from hour to hour within each case.

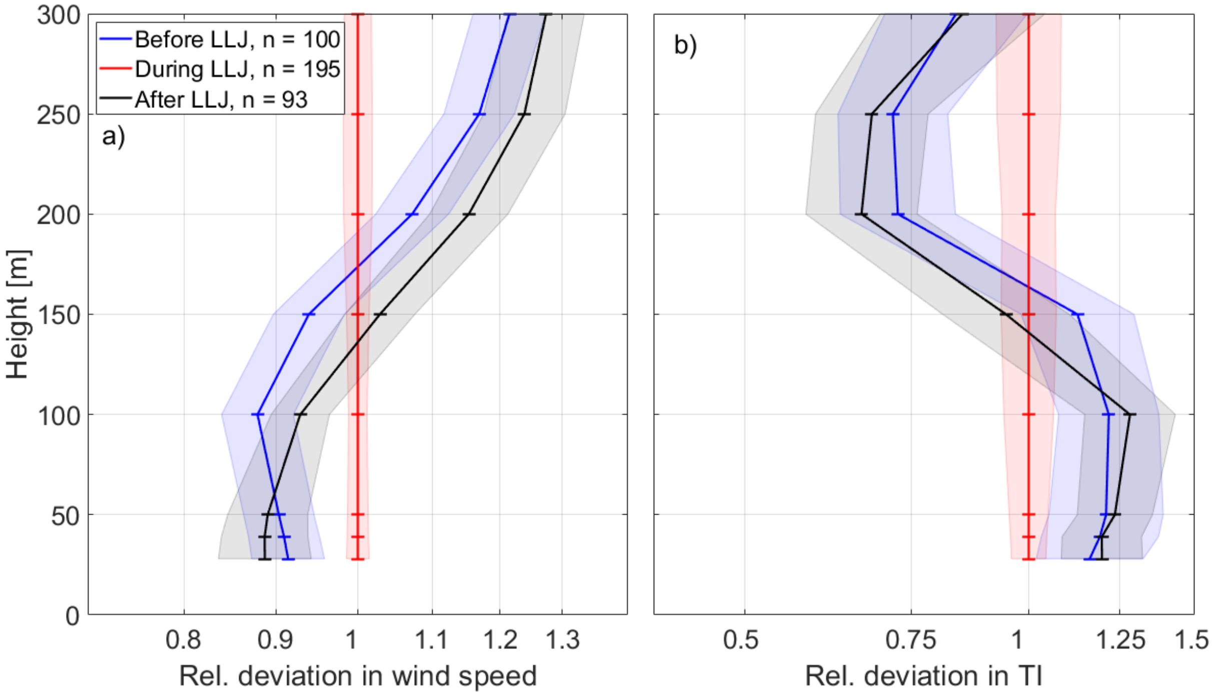

Figure 7. Vertical profile of the normalized mean wind speed (**a**) and normalized mean *TI* (**b**) for before, during and after low-level jets. The shaded area represents a 95% confidence interval, based on assumed Gaussian distributed normalized data. The x-axis is logarithmic and represents the relative deviation from mean *TI* during the LLJs at each height

The vertical profiles of the mean normalized wind speed data can be seen in figure 7a) and the mean normalized *TI* data in figure 7b). The general trend is similar to that of the non-normalized data. As a result of the normalization method, *TI* and wind speed during LLJs is perfectly centered around one. From figure 7a) it is clear that wind speed during the jets is higher below the core and lower above the core. The difference is significant.

The results from figure 7b) are also presented in Table 2, for below and above the core. The distribution of that data is also presented in figure 8. Above the core, mean *TI* before and after LLJs is around 70% of the mean *TI* during the LLJs at 200 and 250 m with clear significant difference. Once again, this shows that as a LLJ forms, *TI* increases in the area above the core, but ones the jets disappear *TI* returns to roughly the same values.

Below the core, there is in general around 20% higher *TI* before and after the jets. In the presence if a LLJ, *TI* below the core decreases, but ones the jet disappear *TI* return to the initial values. However, the confidence interval between before and during the jets is overlapping. The larger confidence interval of the mean *TI* before LLJs is also seen in figure 8b), where before LLJ has a larger spread than after LLJ. In the histogram, once again, the trend of lower *TI* during LLJs below the core can be seen. Figure 8 also show that the normalized data roughly is Gaussian distributed, and that the spread in normalized *TI* is larger above the core (compare figure 8a with 8b).

Table 2. Mean relative deviation from mean *TI* during LLJs for before, during and after LLJs for the two height ranges of interest. The error represents 95% confidence interval

Height [m]	Rel. deviation of $\bar{TI}$ before LLJs	Rel. deviation of $\bar{TI}$ during LLJs	Rel. deviation of $\bar{TI}$ after LLJs
300	0.84 ± 0.15	1.00 ± 0.08	0.85 ± 0.17
250	0.72 ± 0.10	1.00 ± 0.08	0.68 ± 0.09
200	0.73 ± 0.10	1.00 ± 0.07	0.66 ± 0.09
50	1.21 ± 0.17	1.00 ± 0.05	1.23 ± 0.11
38	1.19 ± 0.17	1.00 ± 0.04	1.20 ± 0.12
29	1.16 ± 0.15	1.00 ± 0.04	1.20 ± 0.12

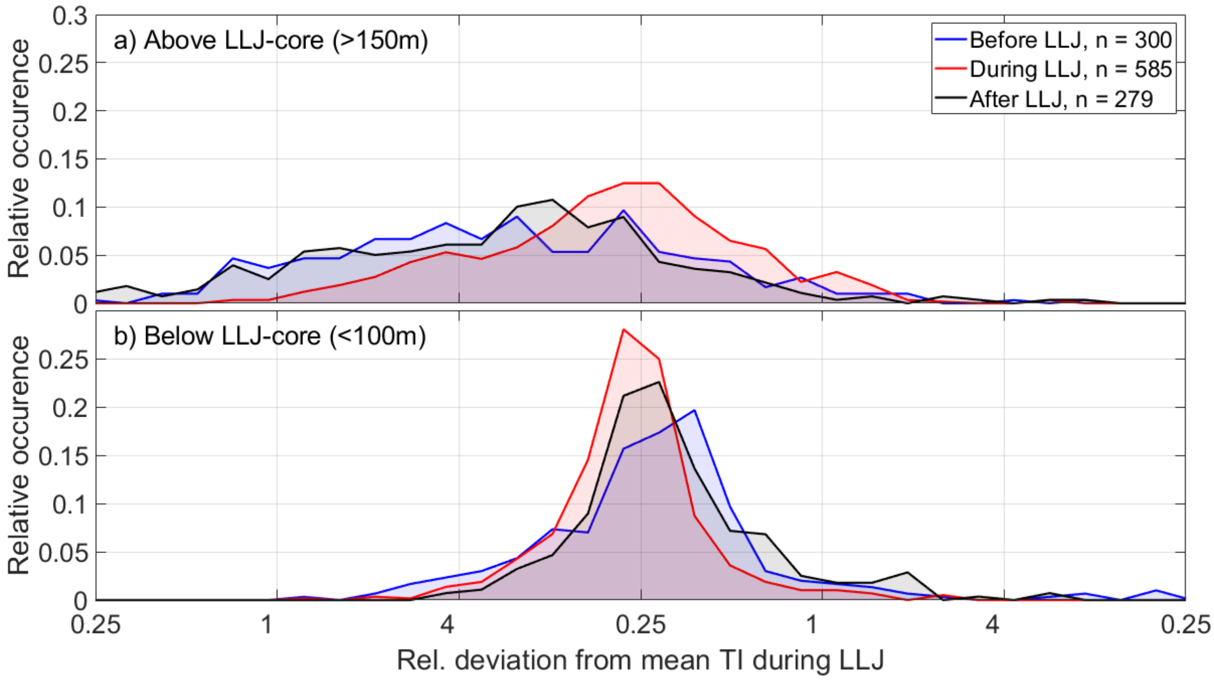

Figure 8. Distribution of normalized *TI* before, during and after LLJ for the range above the core (**a**) and below the core (**b**). The x-axis is logarithmic and represents the relative deviation from mean *TI* during the LLJs at each height with a relative bin size of approximately 0.20

5. Discussion

5.1 Evaluation of the LLJ-finding algorithm

As the identification of LLJs and non-LLJs is essential for this study, this section presents a brief evaluation of the algorithm used and the resulting profiles. As mentioned in section 3.3, the criteria used in this study are relatively low, with a falloff of 1 m/s (if $u_{core} < 10$ m/s) or 10% (if $u_{core} \geq 10$ m/s). Using an absolute criteria for lower wind speeds ensures that variation during calm conditions does not get classified as jets (Tuononen et al. 2017). Using a looser criteria can be justified by the relatively low vertical range in this study, as it is probable that jets would be missed otherwise (Svensson et al. 2019).

Stricter criteria are used by Blackadar (1957), Bonner (1968) (2.5 m/s) and Tuononen et al. (2017), Baas et al. (2009) (2 m/s and 25%) as well as Andreas et al. (2000), Duarte et al. (2012) (2 m/s) while similar criteria are used by Svensson et al. (2019), Hallgren et al. (2020) (1 m/s) and even looser criteria are used by Banta et al. (2002) (both 0.5 and 1 m/s). The application of the criteria vary between the studies, some apply them to all or one point above and below the jet maximum, or only above the core. This study has relatively low vertical resolution, with only eight different height measurements, why it is justified to check for the criteria at only one point above and below the core. This allows for some flexibility when it comes to the vertical extent of the jet core, as well as the profiles behaviour at the highest level.

Identifying non-LLJ profiles before and after a LLJ-event, has to our knowledge not been done before. The criteria and method used for this is therefore - as is the other criteria - rather subjective. The main purpose of the non-LLJ criteria is to exclude LLJ-profiles and transition profiles, and the method does this as visualised in figure 5. The non-LLJ profiles were also manually inspected, which lead to the conclusion that no LLJ profile was identified incorrectly. For future studies the method of identifying non-LLJs before and after a LLJ-event can be optimised, perhaps by fitting the profiles to a log wind profile. Another option would be to skip any additional criteria, and instead look at all profiles before and after that does not meet the LLJ-criteria. This has the benefit of a creating a more representative and larger data set, but it does not exclude transition profiles.

The algorithm finds a lower frequency of LLJ-events compared to other studies from the same study site. Though the yearly and monthly variability is high (Hallgren et al. 2020), studies have found a yearly average LLJ-frequency of approximately 7% (Svensson et al. 2019) to 12% (Hallgren et al. 2020) at Östergarnsholm. This study found an average frequency of 3.3% using similar criteria, and even lower, 1.4%, when applying criteria for complete LLJ-events. Applying more restriction is, of course, expected to decrease the number of events, but the comparably low frequency is probably partly due to two factors regarding the wind direction.

Firstly, LLJs in the Baltic Sea are most common during southeasterly winds (Svensson et al. 2019) which is in the direction of the hut that this study exclude. Secondly, also due to the hut, the wind direction of this data set is limited to two non-continuous sectors, $45 - 110°$ and $150 - 220°$, and any profile that has at at least one point a wind direction outside these ranges is excluded. This, probably, leads to a data set that is not very continuous, since some wind veer is expected within any given profile. Applying some temporal criteria to a non-continuous data set inevitably leads to a rapid decrease in data.

For future studies, this problem can be solved in several ways. Detailed analyses of the hut's effect on *TI* is one of them. If the effect is negligible the problem of a non-continuous wind direction is removed. If this is not the case, some flexibility while removing profiles outside the accepted wind direction, perhaps by allowing one measurement to be outside the range, could lead to a more continuous data set. Another, more obvious, solution would be to choose a study location with a larger, unobstructed view of the ocean.

Applying the threshold minimum of 3 hours transition phase between LLJ-event and non-LLJ profiles may also contribute to the low frequency of complete LLJ-events. Depending on the conditions it is possible that the transition is longer than 3 hours (Blackadar 1957), though further investigation is needed.

5.2 *TI* as a measurement of turbulence

Since *TI* is defined as σ_u/u, it would be expected to measure higher *TI* for lower u and vice verse if σ_u was constant. This is partly the results presented in figure 5 & 7, where lower u is correlated to higher *TI*. However, σ_u is not constant and *TI*'s dependence on u is not that simple. In figure 3, we see a weak $1/u$ dependence for low wind speeds, but for $u > 4$ m/s the trend is more or less constant, or even a slight increase in *TI* with u, especially below the core. The same constant trend is true for the subset of LLJ-data, suggesting that *TI*'s dependence on wind speed in fact is more or less constant within the given wind speed range.

How offshore *TI* depends on wind speed was extensively studied by Türk & Emeis (2010) and they found similar results: at a offshore platform in the North Sea close to Germany, *TI* rapidly decreases with u until approximately $7-9$ m/s; then *TI* slowly increases being more or less constant within the $7-14$ m/s range. The exact values varies depending on height; lower altitudes have minimum *TI* at lower wind speeds and a stronger increase of *TI* as u increases. The authors conclude that increasing offshore *TI* with increasing u after a threshold is due to increasing wave height and surface roughness, which explains why the effect is more obvious closer to the surface.

Both figure 3 and 4 illustrates that the majority of LLJ *TI* measurements are below the median *TI*. This suggests that LLJs, at least found with this study's method, are present during conditions with low *TI*. Very similar figures are presented by Mohr et al. (2018) at different heights, though for turbulence above forests. By comparing the location of the LLJ data in figure 3 to figure 4.3 in Mohr et al. (2018) it is reasonable to conclude that the LLJs mostly are present during stable (or at least neutral) conditions as defined by Mohr et al. (2018). For future studies, a more thorough analysis of the atmospheric stratification during LLJs would be beneficial. Though the exact values of *TI* and u presented by Mohr et al. (2018) is not comparable to this study, they found that *TI* is expected to remain constant with respect to wind speed during neutral and stable conditions. These results are compatible with both Türk & Emeis (2010) and figure 3.

5.3 Characteristics of *TI* above the LLJ-core

In general, above the LLJ-core there is a clear increase in *TI* during LLJs compared to before and after, as presented in section 4.2. This has, to our knowledge, never been presented before. As seen in both figure 5b) and 7b) the difference in *TI* is most noticeable close to the core, suggesting that the jet effects the turbulence and that the effect would diminish as you move further form the core. This could easily be verified in future studies by using a higher vertical limit.

Even though the results are statistically significant at 200 and 250 m, the absolute change in mean *TI* is not that large. The change is approximately 0.010 ± 0.004. Due to low *TI*, as discussed earlier, this still results in a large relative change. The normalized data shows that mean *TI* before the jets is approximately 72 ± 10%, while mean *TI* after is 68 ± 9%, compared to during the jets at 200 and 250 m. In other words, mean *TI* during LLJs increase by roughly $38 - 47$%.

Though the results show that higher *TI* is in general expected during a LLJ-event, this is not true on a case-by-case basis. In fact, in figure 6a,b,c) we see that at least two complete LLJ-events show a decrease in *TI* during the jet. This suggests that there are other factors that also effects the turbulence during the event. For future studies, detailed analysis of these cases with regards to mesoscale conditions, atmospheric stratification and other meteorological variables could provide a more comprehensive pattern. Figure 6 also illustrates that the variation in *TI* within each complete LLJ-event is large.

Once again, it should be noted that the reliability of the turbulence measurements from the ZephIR 300 LiDAR heights above 100 m is uncertain (Svensson et al. 2019). The LiDAR is expected to underestimate *TI* at higher heights due to the larger measurement volume (Sathe et al. 2011), but other studies instead suggest an overestimate (Mohr et al. 2018, Svensson et al. 2019). Regardless if the LiDAR under- or overestimates, the studies all agree that it is a systematic error. This systematic error may effect the absolute values in this height range, but is not expected to effect the results presented by the normalized data, i.e. the relative change.

5.4 Characteristics of *TI* below the LLJ-core

Below the LLJ-core, mean *TI* is slightly lower during the jets, as presented in section 4.2. However, the difference is not as clear compared to above the core. In fact, comparing before and during LLJs we can not say that there is a significant difference with the given 95% confidence interval. This is the case for both the non-normalized and normalized data. While the before and after case show some differences in both wind speed and *TI*, they are both well within each other confidence interval, therefore no difference between them can be concluded. Sacrificing some certainty, we can conclude that mean *TI* decreases below the core in the presence of a LLJ with 90% confidence.

Similar to above the core, the absolute change in mean *TI* is relatively low. At 29 m the difference is approximately 0.006 ± 0.004, and very similar at 38 and 50 m. Once again, due to the generally low *TI* of offshore LLJs, this leads to a large relative change. Mean *TI* before and after the jets is a maximum of 123 ± 11% and a minimum of $116 \pm 15\%$ compared to mean *TI* during the jets in the region below the core. The difference is larger closer to the core, similar to the results above the core. In other words, mean *TI* below the core decreases with roughly $14 - 19\%$ in the presence of LLJs.

The variability of normalized *TI* both between and within each case is lower below compared to above the core, visually seen in figure 8b) and 6d,e,f). This could be due to more stable conditions below the core, but it is difficult to exclude the possibility that the larger measurements volume at higher heights also introduces more random errors (and not only systematic errors as discussed in section 5.3). Figure 6d,e,f) also show that the results of decreased mean *TI* during LLJs not necessarily is true on a case-by-case basis, similar to the results above the core. At least two events have a clear increase in *TI* during LLJs below the core.

5.5 Shear sheltering

The result that *TI* decreases below the core as the low-level jet forms, and then returns to roughly the initial values, is compatible with the theory of shear sheltering. The theory suggests that eddies of certain scale and velocity are prevented from passing through the large shear zone of a LLJ, effectively lowering turbulence below a LLJ core (Hunt & Durbin 1999, Smedman et al. 2004). However, this study does not attempt to explain the mechanism behind the reduced *TI* below the LLJ core, and it is possible that other factors are the reason behind the results. For example, since LLJs often occur due to frictional decoupling (Hallgren et al. 2020) it is possible that lower *TI* is the reason behind the jets and not vice verse as shear sheltering suggest. For future studies, analysis of other turbulent quantities before, during and after LLJs, such as momentum transfer, variance spectra or turbulent kinetic energy, could provide more insight to the reason behind decreased turbulence intensity below a LLJ.

Previous studies analysing shear sheltering during LLJs (Smedman et al. 2004, Prabha et al. 2008, Duarte et al. 2012) have done more in depth analysis of other turbulent quantities. Turbulence intensity below LLJ core is only analysed by Prabha et al. (2008), in which cases with low shear sheltering (classified by a shear sheltering parameter defined by Smedman et al. (2004)) had *TI* of $0.4 - 1$ while cases with high shear sheltering had *TI* of around 0.3. While these results are not comparable to this study's results, since Prabha et al. (2008) analyses onshore LLJs, they do indicate that shear sheltering during LLJs indeed decreases turbulence intensity.

6. Conclusions

Using vertical measurements of wind characteristics from a ZephIR 300 LiDAR located at Östergarnsholm, Gotland, during the period 2016-2020, turbulence intensity during offshore low-level jets is analysed. Firstly, LLJ-events from the sea sector are identified using a 1 m/s and 10% fall off criteria as well as 2.5 hour temporal criteria. The LLJ-events occur with a frequency of 3.3%. Then non-LLJ profiles before and after the jet-events are identified and classified as complete LLJ-events. In total, 19 complete events are identified with jet profiles within a complete LLJ-event occurring 1.4% of the time.

How turbulence intensity depends on wind speed and shear is analysed and the results show that *TI* is more or less constant within the given wind speed range. In general, low *TI* during LLJs suggests that they occur during stable or neutral stratification, which further suggests that *TI* is more or less constant in relation to wind speed.

Finally, the characteristics of *TI* during offshore LLJs is presented. The results show that above the low-level jet core, turbulence intensity increases with around 0.01, or when normalized to the mean *TI* of the jets, an increase of around $38 - 47$ %. On the other hand, below the core, *TI* decreases during the jets with around 0.006, or when normalized, a decrease of around $14 - 19\%$. These results are statistically significant with 95% confidence above the core and 90% below the core. The decrease of turbulence intensity below the core of a LLJ is compatible with the theory of shear sheltering, though this study does not attempt to explain the exact mechanisms behind the results. However, within any individual event, the *TI* measurements are highly variable and there are events in which the results are opposite or not seen at all.

For future studies optimising the algorithm used to find complete LLJ-events is preferable, especially when it comes to identifying non-LLJ profiles before and after an event. Another recommendation is to choose a study location with a larger unobstructed line-of-sight to the ocean and using a longer time series, leading to more complete LLJ-events being identified. Another recommendation is to analyse atmospheric stratification and weather conditions during each event which could explain the reasons for some events showing different results. Finally, to further draw conclusions regarding shear sheltering and turbulence during LLJs, analyses of other turbulent quantities would be beneficial.

Acknowledgements

I wish to thank all the people who made this project possible, especially my supervisor, Christoffer Hallgren. His knowledge within the field has been valuable, and his assistance throughout the project, while planning, executing the analysis and writing the thesis is greatly appreciated. I also want to thank Erik Sahlée, my subject reviewer, as well as other employees at the Department of Earth Sciences at Uppsala University for interesting discussions and feedback.

The Östergarnsholm site is a part of the ICOS (Integrated Carbon Observation Study) and is funded by Swedish Research Council and Uppsala University. Technical staff working at the Östergarnsholm station are greatly acknowledged.

References

Andreas, E., Claffy, K. & Makshtas, A. (2000), 'Low-Level Atmospheric Jets And Inversions Over The Western Weddell Sea', *Boundary-Layer Meteorology* **97**.

Baas, P., Bosveld, F. C., Baltink, H. K. & Holtslag, A. A. M. (2009), 'A Climatology of Nocturnal Low-Level Jets at Cabauw', *Journal of Applied Meteorology and Climatology* **48**(8), 1627 – 1642.

Banta, R., Newsom, R., Lundquist, J., Pichugina, Y., Coulter, R. & Mahrt, L. (2002), 'Nocturnal Low-level Jet Characteristics over Kansas during CASES-99'. Boundary-Layer Meteorol. 105, 221-252', *Boundary-Layer Meteorology* **105**, 221–252.

Bilgili, M., Yasar, A. & Simsek, E. (2011), 'Offshore wind power development in Europe and its comparison with onshore counterpart', *Renewable and Sustainable Energy Reviews* **15**(2), 905–915.

Blackadar, A. K. (1957), 'Boundary Layer Wind Maxima and Their Significance for the Growth of Nocturnal Inversions', *Bulletin of the American Meteorological Society* **38**(5), 283 – 290.

Bonner, W. D. (1968), 'Climatology of the Low Level Jet', *Monthly Weather Review* **96**(12), 833 – 850.

Brandt, L., Schlatter, P. & Henningson, D. S. (2004), 'Transition in boundary layers subject to free-stream turbulence', *Journal of Fluid Mechanics* **517**, 167–198.

Duarte, H., Leclerc, M. & Zhang, G. (2012), 'Assessing the shear-sheltering theory applied to low-level jets in the nocturnal stable boundary layer', *Theor Appl Climatol* **110**.

Dörenkämper, M., Witha, B., Steinfeld, G., Heinemann, D. & Kühn, M. (2015), 'The impact of stable atmospheric boundary layers on wind-turbine wakes within offshore wind farms', *Journal of Wind Engineering and Industrial Aerodynamics* **144**, 146–153.

Hallgren, C., Arnqvist, J., Ivanell, S., Körnich, H., Vakkari, V. & Sahlée, E. (2020), 'Looking for an Offshore Low-Level Jet Champion among Recent Reanalyses: A Tight Race over the Baltic Sea', *Energies* **13**(14).

Hernon, D., Walsh, E. J. & McEligot, D. M. (2007), 'Experimental investigation into the routes to bypass transition and the shear-sheltering phenomenon', *Journal of Fluid Mechanics* **591**, 461–479.

Holt, T. (1996), 'Mesoscale forcing of a boundary layer jet along the California coast', *Journal of Geophysical Research* **101**, 4235–4254.

Hunt, J. & Durbin, P. (1999), 'Perturbed vortical layers and shear sheltering', *Fluid Dynamics Research* **24**(6), 375 – 404.

Jacobs, R. G. & Durbin, P. A. (2001), 'Simulations of bypass transition', *Journal of Fluid Mechanics* **428**, 185–212.

Kaellstrand, B. (1998), 'Low level jets in a marine boundary layer during spring', *Contributions to Atmospheric Physics* **71**.

Mohr, M., Arnqvist, J., Abedi, H., Alfredsson, H., Baltscheffsky, M., Bergström, H., Carlen, I., Davidson, L., Antonio, S. & Söderberg, S. (2018), Wind Power in Forests II, Technical report.

Nagarada Gadde, S. & Stevens, R. J. A. M. (2020), 'Interaction between low-level jets and wind farms in a stable atmospheric boundary layer', *arXiv e-prints* p. arXiv:2001.11919.

Parish, T. (2000), 'Forcing of the Summertime Low-Level Jet along the California Coast', *Journal of Applied Meteorology* **39**, 2421–2433.

Prabha, T., LeClerc, M., Karipot, A., Hollinger, D. & Mursch, E. (2008), 'Influence of Nocturnal Low-level Jets on Eddy-covariance Fluxes over a Tall Forest Canopy', *Boundary-Layer Meteorology* **126**.

Ramírez, L., Fraile, D. & Brindley, G. (2020), Offshore Wind in Europe: Key Trends and Statistics 2020, Technical report, Brussels, Belgium.

Rutgersson, A., Pettersson, H., Nilsson, E., Bergström, H., Wallin, M. B., Nilsson, E. D., Sahlée, E., Wu, L. & Mårtensson, E. M. (2020), 'Using land-based stations for air–sea interaction studies', *Tellus A: Dynamic Meteorology and Oceanography* **72**(1), 1–23.

Sathe, A., Mann, J., Gottschall, J. & Courtney, M. (2011), 'Can Wind Lidars Measure Turbulence?', *Journal of Atmospheric and Oceanic Technology* **28**, 853–868.

Smedman, A.-S., Högström, U. & Bergström, H. (1997), 'The turbulence regime of a very stable marine airflow with quasi-frictional decoupling', *Journal of Geophysical Research: Oceans* **102**(C9), 21049–21059.

Smedman, A.-S., Högström, U. & Hunt, J. C. R. (2004), 'Effects of shear sheltering in a stable atmospheric boundary layer with strong shear', *Quarterly Journal of the Royal Meteorological Society* **130**(596), 31–50.

Svensson, N., Arnqvist, J., Bergström, H., Rutgersson, A. & Sahlée, E. (2019), 'Measurements and Modelling of Offshore Wind Profiles in a Semi-Enclosed Sea', *Atmosphere* **10**(4).

Swedish wind energy association (2019), 100 percent renewable electricity by 2040, Technical report, Stockholm, Sweden.

Tuononen, M., O'Connor, E. J., Sinclair, V. A. & Vakkari, V. (2017), 'Low-Level Jets over Utö, Finland, Based on Doppler Lidar Observations', *Journal of Applied Meteorology and Climatology* **56**(9), 2577 – 2594.

Türk, M. & Emeis, S. (2010), ‘The dependence of offshore turbulence intensity on wind speed’, *Journal of Wind Engineering and Industrial Aerodynamics* **98**(8), 466–471.


S. ACADEM
ATIAE
RITAS